

Excavation rate of silicon surface nanoholes

Yutaka Ohno^{a)} and Seiji Takeda

Department of Physics, Graduate School of Science, Osaka University, 1-1 Machikane-yama, Toyonaka, Osaka 560-0043, Japan

Toshinari Ichihashi

Fundamental Research Laboratories, NEC Corporation, 34 Miyukigaoka, Tsukuba, Ibaraki 305-8501, Japan

Sumio Iijima

Fundamental Research Laboratories, NEC Corporation, 34 Miyukigaoka, Tsukuba, Ibaraki 305-8501, Japan and Meijo University, 1-501 Shiogamaguchi, Tenpaku-ku, Nagoya 468-8502, Japan

(Received 31 January 2006; accepted 4 April 2006; published online 27 June 2006)

Silicon surface nanoholes, that are small pits introduced spontaneously on electron exit surfaces of silicon foils under electron irradiation, are excavated at a constant rate with increasing electron dose. On the other hand, surface nanoholes on electron entrance surfaces become shallow under electron irradiation. The mechanism for the excavation and shallowing of surface nanoholes is discussed in terms of the movement of surface vacancies assisted by irradiating electrons. © 2006 American Institute of Physics. [DOI: 10.1063/1.2206693]

Arrays of one-dimensional nanostructures, i.e., nanoholes, nanotubes and nanowires, etc., on surfaces have attracted considerable attention because of their potential utilization in future nanodevices. Among them, surface nanohole arrays may be applied to optoelectronic devices, such as photonic waveguides and plasmonic integrated circuits,¹⁻³ and also they can be used as templates for the fabrication of useful nanostructures.⁴⁻⁶ Surface nanohole arrays can be formed by spontaneous fabrication techniques such as electron irradiation,⁷ electrochemical etching,⁸ etc., which have advantages in comparison with artificial techniques such as electron lithography,^{9,10} even though the formation mechanism is not fully understood. Here, surface nanohole arrays in silicon, formed spontaneously on electron exit surfaces of silicon foils under electron irradiation,⁷ are examined. They distribute orderly in a short range, and the two-dimensional patterning is explained quantitatively in terms of the migration of surface vacancies under electron irradiation.¹¹ However, the excavation mechanism has not been elucidated. In this paper, the mechanism is studied by transmission electron microscopy (TEM) at an ultrahigh vacuum (UHV) and related techniques, since controlled clean surfaces can be provided and the formation of nanostructures on the surfaces, on which an arbitrary number of point defects are introduced intentionally, can be pursued. The excavation rate of surface nanoholes is estimated systematically, and the mechanism is discussed in terms of the movement of surface vacancies assisted by irradiating electrons.

Samples were thin foils of nondoped Czochralski {001} silicon wafers, unless it is noted in the text. Nanoholes were formed on a clean deoxidized surface in an UHV microscope (the base pressure P_{ir} of about 1×10^{-7} Pa) or a surface virtually deoxidized in a conventional microscope¹² ($P_{\text{ir}} \sim 1$

$\times 10^{-5}$ Pa) by electron irradiation. The irradiation direction was normal to the surface, unless it is noted in the text. The electron flux f was up to about 5×10^{21} $e \text{ cm}^{-2} \text{ s}^{-1}$, and the electron energy E_{ir} was up to 200 keV. The electron dose D , f multiplied by the irradiation time t , was up to about 2×10^{24} $e \text{ cm}^{-2}$. The nominal temperature during irradiation T_{ir} ranged from room temperature (RT) to about 680 K in an UHV microscope and from about 4 to 680 K in a conventional microscope. The irradiated surface was then observed by TEM with electrons of low flux, so that the surface was virtually kept unchanged during observation.¹³

The distribution of surface nanoholes is determined at the early stage of irradiation,¹⁴ and a nanohole is excavated, parallel to the irradiation direction, without changing the size of the opening under irradiation.⁷ Therefore, only the excavation process, characterized by the depths, is taken into account after the formation of two-dimensional patterns of the nanoholes. The depths of surface nanoholes can be estimated by means of three-dimensional TEM [e.g., Figs. 1(a) and 1(b)], and so the excavation process can virtually be pursued [e.g., Figs. 1(b)–1(d)]. Figure 1(f) shows the typical excavation process. The depths of surface nanoholes at an electron dose are slightly dispersed [e.g., Fig. 1(e)], and so each depth is plotted. As seen in the figure, surface nanoholes are excavated at a constant rate with increasing D .

Taking the above-mentioned result into account, the excavation rate of surface nanoholes R can be estimated by *in situ* TEM. A theoretical calculation suggested that a surface nanohole is observable by TEM when the depth is more than about 3 nm. Actually, even though shallow surface nanoholes (less than 2 nm deep) are formed by the irradiation with electrons of low dose (less than 2×10^{23} $e \text{ cm}^{-2}$), they are hardly observable by TEM.¹⁴ Surface nanoholes are excavated with increasing D , and they become visible by TEM when D reaches a specific value of D_{min} . Therefore, the excavation rate is estimated that $R \sim 3/D_{\text{min}}$ in $\text{nm}/(e \text{ cm}^{-2})$. R

^{a)}Electronic mail: ohno@phys.sci.osaka-u.ac.jp

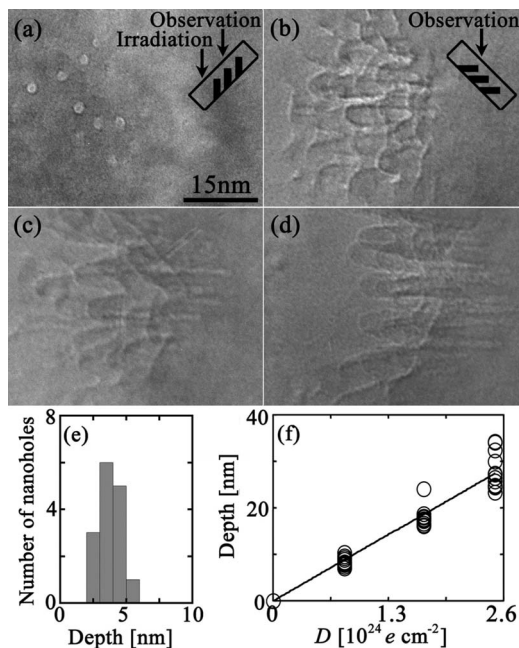


FIG. 1. Surface nanoholes formed by electron irradiation for t = [(a) and (b)] 180, (c) 360, and (d) 540 s ($P_{ir} \sim 1 \times 10^{-5}$ Pa, $f = 4.6 \times 10^{21} e \text{ cm}^{-2} \text{ s}^{-1}$, $T_{ir} = \text{RT}$). They are observed (a) parallel to and [(b)–(d)] normal to the irradiation direction. The irradiation direction was about 45° degrees inclined from [001], as schematically shown in (a). (e) The distribution of the depths of the nanoholes in (b). (f) D dependence of the depths of surface nanoholes.

for the surface nanoholes formed with the same experimental condition as in Fig. 1 was estimated by this method [about $1 \text{ nm}/(10^{23} e \text{ cm}^{-2})$], and the estimated value really corresponded to the excavation rate estimated in Fig. 1(f) [$1.2 \text{ nm}/(10^{23} e \text{ cm}^{-2})$].

R was independent of f at an UHV when E_{ir} and T_{ir} were fixed [e.g., Fig. 2(a)]. When P_{ir} was increased, R decreased with decreasing f and no surface nanohole was formed when f was low [e.g., the broken curve in Fig. 2(b)], due to effects of oxidation⁷ and contamination. R was independent of P_{ir} at

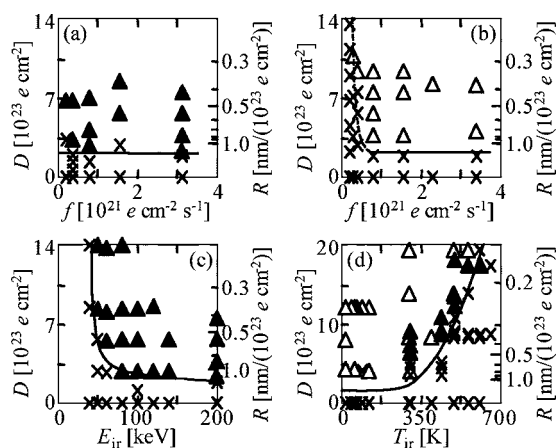


FIG. 2. Diagrams of the steady state of electron exit surfaces. Crosses mean that surface nanoholes are invisible, while triangles mean that surface nanoholes are observable by TEM [$P_{ir} \sim 1 \times 10^{-7}$ Pa (closed triangles) or $\sim 1 \times 10^{-5}$ Pa (open triangles)]. The solid line in each figure denotes a theoretical calculation of R from Eqs. (1) and (2) ($\gamma = 0.05$). (a) and (b) are R vs f at different P_{ir} ($E_{ir} = 200 \text{ kV}$, $T_{ir} = \text{RT}$). (c) R vs E_{ir} at $T_{ir} = \text{RT}$ and (d) R vs T_{ir} at $E_{ir} = 200 \text{ kV}$ ($f = 3.2 \times 10^{21} e \text{ cm}^{-2} \text{ s}^{-1}$).

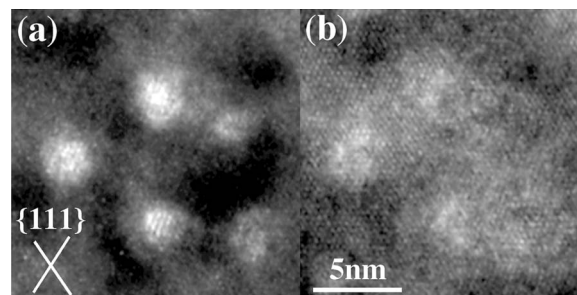


FIG. 3. Shallowing nanoholes on an electron entrance surface. Nanoholes were first formed on a (110) surface with the irradiation direction of [110] ($P_{ir} \sim 1 \times 10^{-5}$ Pa, $T_{ir} = \text{RT}$, $D = 1.6 \times 10^{24} e \text{ cm}^{-2}$). The specimen was turned over and then irradiated with the irradiation direction of $[\bar{1}\bar{1}0]$. $D =$ (a) 0.0 and (b) $5.1 \times 10^{23} e \text{ cm}^{-2}$.

high f [Figs. 2(a) and 2(b)], and this clearly indicates that the surfaces irradiated with electrons of high flux are virtually free from oxidation and contamination even at low vacuum.¹² In the high flux range, R decreased with decreasing E_{ir} and no surface nanohole was formed when E_{ir} was below about 40 keV [e.g., Fig. 2(c)]. Also, R decreased with increasing T_{ir} and no surface nanohole was formed when T_{ir} was above about 600 K [e.g., Fig. 2(d)].

Vacancies are introduced on electron entrance surfaces, as well as on electron exit surfaces, by irradiation with high-energy electrons and they would aggregate on the surfaces via their migration under electron irradiation.¹⁵ However, nanoholes on electron entrance surfaces became shallow by electron irradiation (Fig. 3). This indicates that surface vacancies on electron exit surfaces flow into nanoholes while those on electron entrance surfaces flow out nanoholes under electron irradiation.

One possible mechanism for the excavation and shallowing of surface nanoholes is the flow of surface vacancies due to the momentums transferred from irradiating electrons⁷ [Fig. 4(a)]. Suppose a surface vacancy reaches the edge of a nanohole on an electron exit surface, via its migration on the surface. The vacancy may exchange its position with a nearby atom due to the momentum transfer mechanism,¹⁷ when the atom is transferred a momentum from an irradiating electron. As a result, the vacancy moves opposite to the direction of the movement of the atom transferred momentum. Since the intensity of transferred momentum is high when the direction of the momentum is near the irradiation direction, the vacancy preferentially moves opposite to the irradiation direction and so the nanohole is excavated paral-

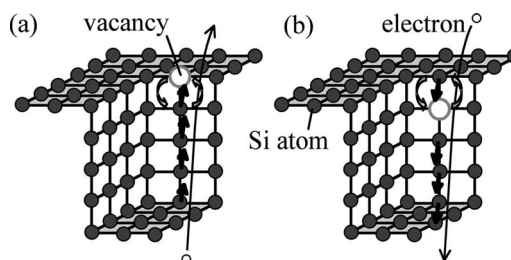


FIG. 4. Schematic view of the (a) excavation or (b) infilling process of surface nanohole. The closed thick arrows denote the momentums of silicon atoms transferred from the irradiating electron.

lel to the irradiation direction under electron irradiation. On the contrary, surface vacancies in nanoholes on electron entrance surfaces preferentially flow out under electron irradiation due to the similar effect [Fig. 4(b)]. As a result, atoms preferentially flow into the nanoholes from the initial surface, so as to infill the nanoholes, under electron irradiation.

According to the above-mentioned model, we discuss the excavation rate of surface nanoholes.¹⁸ The number of vacancies on an irradiated surface may be estimated with the standard theory for radiation damage in materials.²⁰ The displacement damage on a surface leaves vacancies, and the number of surface vacancies introduced per an irradiated area is $\gamma\sigma(E_{\text{ir}})D$. $\sigma(E_{\text{ir}})$ is the cross section of displacement damage for a surface atom,²¹ and γ is a constant.²⁴ Among them, $\alpha(0 \leq \alpha \leq 1)$ of the vacancies aggregate into nanoholes, and the rest fill up the initial surface.¹⁴ As a result, $\alpha\gamma\sigma(E_{\text{ir}})D = nSd/d_{\text{mono}}$, where d is the mean depth of surface nanoholes and d_{mono} is the height of a monolayer step (about 0.1 nm). n and S are the areal number density and the mean opening area of surface nanoholes, respectively, and nS is estimated to be about 0.1.¹¹ The excavation rate can be, therefore, written as

$$R = d/D = \alpha\gamma\sigma(E_{\text{ir}})d_{\text{mono}}/nS. \quad (1)$$

α may be related to the mobility of surface vacancies including the momentum transfer effect, and it should depend on T_{ir} and E_{ir} on deoxidized surfaces.²⁶ It is suggested that²⁰ vacancies introduced by irradiation can aggregate, via their thermal migration, and the number of the vacancies that aggregate per unit electron dose is in proportion to $M^{0.5}$, in which M is the coefficient for the thermal migration of vacancies. In this study, vacancies could migrate thermally only on surfaces¹⁵ and so the number of the vacancies that fill up the initial surface per unit electron dose can be written as $AM^{0.5}$, in which A is a constant. The number of the vacancies that flow into nanoholes per unit electron dose is dominated by the movement of surface vacancies due to the momentum transfer effect, and so the number should depend on E_{ir} . As a rough approximation, the number is assumed to be BE_{ir} in which B is a constant. Therefore, α can be written as $BE_{\text{ir}}/(BE_{\text{ir}} + AM^{0.5})$. Since α is estimated to be (0.5 ± 0.2) when $E_{\text{ir}} = 160$ kV at $T_{\text{ir}} = \text{RT}$ (Ref. 14) and M is in proportion to $\exp[-(0.3 \pm 0.04) \text{ eV}/kT_{\text{ir}}]$,¹¹ one can obtain

$$\alpha \sim E_{\text{ir}}/[E_{\text{ir}} + (5 \pm 3) \times 10^4 \exp[-(0.15 \pm 0.02) \text{ eV}/kT_{\text{ir}}]]. \quad (2)$$

The model reproduces well the experimental results with an adequate value²¹ of $0.03 \leq \gamma \leq 0.2$ (e.g., the solid lines in Fig. 2).

In conclusion, silicon surface nanoholes are excavated at a constant rate with increasing electron dose, via the movement of surface vacancies due to the momentum transfer effect. Surface nanoholes with any depth, that can be formed at any position on surfaces, may be used for base materials for nanodevices, templates for designing nanostructures on surfaces with a variety of functions, etc. The results will be a principle of nanofabrication on surfaces by electron irradiation.

This work was partially supported by the Ministry of Education, Culture, Sports, Science, and Technology, Grant-in-Aid for Scientific Research (A) (2) No. 10305006, 2003–2006, and Grant-in-Aid for Young Scientist (A) (2) No. 15681006, 2003–2005.

¹J. B. Pendry, L. Martin-Moreno, and F. J. Garcia-Vidal, *Science* **305**, 847 (2004).

²R. Gordon, A. G. Brolo, A. McKinnon, A. Rajora, B. Leathem, and K. L. Kavanagh, *Phys. Rev. Lett.* **92**, 037401 (2004).

³D. S. Kim *et al.*, *Phys. Rev. Lett.* **91**, 143901 (2003).

⁴Y. Lei, W. K. Chim, H. P. Sun, and G. Wilde, *Appl. Phys. Lett.* **86**, 103106 (2005).

⁵N. Yasui, A. Imada, and T. Den, *Appl. Phys. Lett.* **83**, 3347 (2003).

⁶R. Songmuang, S. Kiravittaya, and O. G. Schmidt, *Appl. Phys. Lett.* **82**, 2892 (2003).

⁷For example, S. Takeda, K. Koto, S. Iijima, and T. Ichihashi, *Phys. Rev. Lett.* **79**, 2994 (1997), and references therein.

⁸For example, Y. Li, Y. Kanamori, and K. Hane, *Microsyst. Technol.* **10**, 272 (2004).

⁹N.-W. Liu, A. Datta, C.-Y. Liu, C.-Y. Peng, H.-H. Wang, and Y.-L. Wang, *Adv. Mater. (Weinheim, Ger.)* **17**, 222 (2005).

¹⁰Y. Awad *et al.*, *J. Vac. Sci. Technol. A* **22**, 1040 (2004).

¹¹Y. Ohno, S. Takeda, T. Ichihashi, and S. Iijima (unpublished).

¹²On surfaces in a conventional microscope, the sputtering of surface atoms, oxidization, and contamination take place simultaneously under electron irradiation. When f is high, the first process is most probably predominant and so the surface is virtually free from oxidization and contamination (Ref. 11).

¹³The flux was about $10^{19} \text{ e cm}^{-2} \text{ s}^{-1}$, and the irradiated surface received electrons of $D \sim 10^{20} \text{ e cm}^{-2}$ throughout TEM observation. The dose needed for observation was much smaller than that for irradiation (above about $10^{23} \text{ e cm}^{-2}$).

¹⁴N. Ozaki, Y. Ohno, M. Tanbara, D. Hamada, J. Yamasaki, and S. Takeda, *Surf. Sci.* **493**, 547 (2001).

¹⁵It is known that vacancies are introduced inside the crystal at $T_{\text{ir}} = \text{RT}$ by the irradiation of electrons whose energy is above 140–150 keV (Ref. 16). This indicates that the migration of surface vacancies, that can be introduced by the irradiation of electrons with lower energy (down to about 40 keV), toward the inside of the crystal could be negligible. Also, even when E_{ir} is above 140–150 keV, effects of the vacancies inside the crystal could be negligible in the present work, since the number density of vacancies introduced inside the crystal is small (less than 1/30 of the number density on the surfaces even at $E_{\text{ir}} = 200$ keV).

¹⁶J. J. Loferski and P. Pappaport, *Phys. Rev.* **111**, 432 (1958).

¹⁷K. Urban and A. Seeger, *Philos. Mag.* **30**, 1395 (1974).

¹⁸We do not discuss quantitatively the infilling rate of surface nanoholes in the present study, since the number of surface vacancies introduced per an area on an electron entrance surface is unclear. It is considered that the number is rather small for flat electron entrance surfaces hit normally by electrons. However, it is proposed that many surface vacancies are introduced on real electron entrance surfaces irradiated by high-energy electrons (Ref. 19), presumably due to effects of steps existed on the surfaces.

¹⁹K. Torigoe, T. Ichihashi, and S. Takeda (unpublished).

²⁰M. Kiritani and H. Takata, *J. Nucl. Mater.* **69–70**, 277 (1978).

²¹ $\sigma(E_{\text{ir}})$ for a surface can be estimated, with the threshold energy for formation of vacancies on the surface, with the McKinley-Feshbach's formula (Ref. 22). The threshold energy is estimated to be 3.2–4.0 eV (Ref. 11), and it is close to the sublimation energy of a silicon surface [e. g., 3.5 eV for a (111) surface (Ref. 23)].

²²W. A. McKinley and H. Feshbach, *Phys. Rev.* **74**, 1759 (1948).

²³K. Yagi, *Scan Electron Microsc.* **1982**, 1421 (1982).

²⁴The phenomenological parameter $(1-\gamma)$, that is so called a correlated recombination factor, describes the probability that a displaced atom returns to the vacant site from which it originates. γ for displacement of atoms in semiconductors is the order of 10^{-1} (Ref. 25).

²⁵For example, N. Noda and S. Takeda, *Phys. Rev. B* **53**, 7197 (1996).

²⁶Since R is independent of f at an UHV [Fig. 2(a)], α is independent of f on deoxidized surfaces. α may depend on f when f is low at a low vacuum [Fig. 2(b)], due to effects of oxidization and contamination. The effects are ignored in this paper.